6 Studies of spin-coated polymer films

K. Norrman,* A. Ghanbari-Siahkali and N. B. Larsen
DOI: 10.1039/b408857n

Spin-coating is widely employed for the highly reproducible fabrication of thin film coatings over large areas with high structural uniformity. Research in recent years has extended the scope of spin-coating by chemically engineering the interface of support and solution to obtain specific structural order in the resulting supported thin films. This review will discuss both the fundamental physical and chemical processes governing the conventional spin-coating process and describe methodologies for the preparation of spin-coated polymer thin films. Furthermore, a range of advanced applications and recent developments within this field will be reviewed with focus on engineering chemical and topological structure during the coating process.

1 Introduction

The process of applying a solution to a horizontal rotating disc, resulting in ejection and evaporation of the solvent and leaving a liquid or solid film, is called spin-coating, and has been studied and used since the beginning of the 20th century. Spin-coating is a unique technique in the sense that it is possible to apply a highly uniform film to a planar substrate over a large area ($Ø \geqslant 30$ cm) with a highly controllable and reproducible film thickness. The importance of spin-coating is manifested in its widespread use in science and industry. It is thus desirable to gain detailed understanding of the spin-coating process from both an experimental and a theoretical point of view. The spin-coating technique applies to both inorganic, organic and inorganic/organic solution mixtures. However, this review will focus only on spin-coating of polymer films.

Spin-coating is used in various applications such as coating of photoresist on silicon wafers, sensors, protective coatings, paint coatings, optical coatings and membranes.

The most widespread use of the spin-coating technique is for microelectronics applications.[1–15] Silicon is patterned photolithographically with a circuit design by coating semiconductor wafers with a polymeric photoresist film that is subsequently exposed through masks to transfer the circuit design. The coating of polymeric photoresist is applied by the process of spin-coating. Some of the most widely used polymers in microelectronics (and photonics) are photon or electron curable/degradable polymers (for lithographic patterning) and polyimides (*e.g.* for packaging, interlayer dielectrics and flexible circuit boards). For the latter applications in microelectronics, it is desirable to have low dielectric constants, good adhesion and good thermal and mechanical properties.

In the area of sensors there has been much focus on spin-coating of polymer films in recent years.[16–19] For example, because of the hygroscopic properties of many

Danish Polymer Centre, Risø National Laboratory, P.O. Box 49, DK-4000 Roskilde, Denmark

polymers they have proven to be applicable in the field of relative humidity sensing, which have practical applications in the fields of medicine, meteorology, agriculture and process control. Furthermore, the field of oxygen sensors has attracted a lot of attention. The polymer is often mixed with a species that directly or indirectly produces a response and then spin-coated to produce a polymer film. The polymer normally acts as an encapsulating agent in sensor devices. The response from the sensor film is typically based on optical properties, redox chemistry, biological or synthetic oxygen binders, or combinations of these examples.

Protective coatings are widely used in industrial applications, *e.g.* against corrosion, UV light, humidity and scratching.[20] One of the extensive applications is spin-coating of organic dye polymers used as coatings in media for optical data mass storage. A metal layer (gold, silver, copper or aluminium) is applied in order to reflect the laser light, and a thin layer of acrylic plastic is applied by spin-coating for scratch protection. Finally, an extra protective or printer-friendly coating is then applied by spin-coating.

One of the first applications of spin-coating was the application of paint coatings to various industrial products.[21] However, this process was/is limited to products with planar surfaces. A paint coating is often not just cosmetic, but also acts as a protective coating.

The area of optical coatings is versatile and contains many applications were spin-coating plays an important role.[22] Optical coatings with low-refractive indices are used in anti-reflection applications to improve light transmission in industrial and scientific instruments as well as in everyday optical applications. There is still much interest in optimizing broadband antireflection coatings, but the progress is hindered by the of lack of materials with sufficiently low refractive indices. In recent years, fluorine-containing polymers with refractive indices approaching that of water and also suitable for spin-coating has become commercially available but their wider application awaits reduction in material costs.

Spin-coated polymer films that function as membranes have applications in the above mentioned sensor applications, where the polymer film acts as an encapsulating agent and as a barrier layer.[16–19] Ion-exchange membranes are also used as sensors through their engineered contents of ionic functional groups, which can react and/or be coupled with analytes, resulting in a membrane response.[18] Polymer membranes can also be manufactured from a microsphere suspension in a solution of polymer, which is then spin-coated (or more commonly molded) and subsequently polymerized or cross-linked to form a hydrogel.[23] Porous polymer membranes can be formed by spin-coating incompatible polymer blends that will phase-separate during the drying process.[24] A porous polymer film results from the selective dissolution of one of the polymers. The ability to form ever-smaller, monodisperse pores has widened the applications to even more advanced applications, such as separation of enantiomers or biomolecules, drug delivery and catalysis.

2 Theory

The spin-coating process

Depositing a viscous fluid on a horizontal rotating disc produces a uniform liquid film. During deposition the disc should either be static or be rotating at a low angular velocity, where after the disc is rapidly accelerated to a high angular velocity (spin

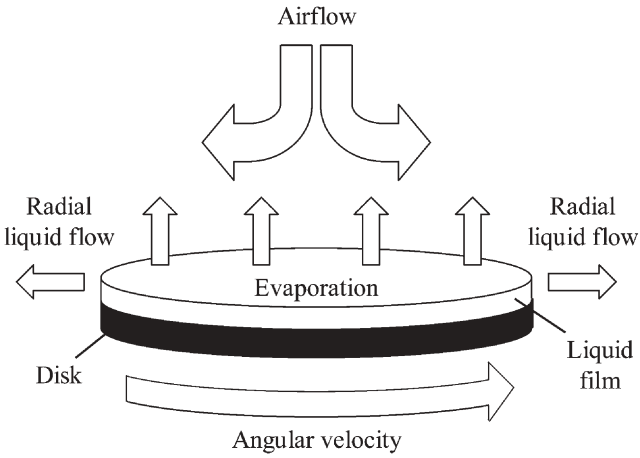

Fig. 1 Schematic of the major spin-coating processes.

speed). The adhesive forces at the liquid/substrate interface and the centrifugal forces acting on the rotating liquid result in strong sheering of the liquid which causes a radial flow in which most of the polymer solution is rapidly ejected from the disc, Fig. 1. This process combined with subsequent evaporation of the liquid causes the thickness of the remaining liquid film to decrease. For a solution, *e.g.* a polymer solution, the evaporation process causes the polymer concentration to increase (and thus the viscosity) at the liquid/vapor interface, *i.e.* a concentration gradient is formed through the liquid film, which, after evaporation of most of the remaining solvent, consequently results in the formation of a uniform practically solid polymer film.

Modelling

The spin-coating process is complex in nature due to the many mechanisms involved. It is thus not straightforward to model the spin-coating process, and it is therefore not surprising that many assumptions and approximations has been applied when attempting to model the process.[25–31] Emslie *et al.*[25] were the first to describe the spin-coating process theoretically. The authors assumed a Newtonian behavior of the fluid (*i.e.* a linear relationship between shear stress and shear rate). Coriolis forces, gravitational gradients, as well as spatial and temporal variations in concentration, viscosity and vertical diffusivity were all neglected. In spite of these crude approximations Emslie *et al.*[25] could make generalized predictions of the flow pattern and the thickness of the resulting films. Later studies by other workers accounted for these disregarded parameters resulting in significantly improved models in better agreement with experimental observations.[32–37]

A great deal of experimental work described in the literature deals with deducing empirical correlations between experimental parameters and film thickness.[27,28,31,38–45] It is thus known that angular velocity, solution viscosity and solution concentration significantly affect the film thickness, and that the amount of solution initially deposited on the disc, the rate at which it is deposited, the history of rotational acceleration prior to the final acceleration, and the total spin time have limited or no effects.

Angular velocity, concentration and viscosity. For a polymer solution the concentration is related to the viscosity, *i.e.* the viscosity increases for higher concentrations (typically not linearly). The angular velocity and concentration (or viscosity) have typically been correlated to the film thickness in the literature.[36,37] The relationship is schematically shown in Fig. 2.

This generalized correlation is a widely observed experimental result, and it is therefore generally accepted that the (empirically derived) mathematical relationship has the following form:

$$h = k_1\omega^{\alpha} \tag{1}$$

where h is the film thickness, ω is the angular velocity, while k_1 and α are empirically determined constants. Fig. 2 shows that for higher angular velocities the film thickness will decrease, and that for lower concentrations (at a given angular velocity) the film thickness will also decrease. The constants, k_1 and α, are dependent on various parameters, including physical properties of the polymer, the solvent, and the substrate, polymer/solvent interactions and solution/substrate interactions, and thus also rheological properties.

The exponent, α, has been observed to change only slightly for various polymer/solvent systems, and has, by most workers, been set in close vicinity of -0.5.[32,36,38–40,41,43] According to Lawrence[37] the deviation from -0.5 observed in some work can originate from several contributing factors. If the spin-coating process is stopped before the radial flow is completed the result would be a thicker film at lower angular velocities, *i.e.* causing the derived exponent to be more negative ($\alpha < -0.5$). Another possible factor causing $\alpha < -0.5$ could be shear thinning, which is more significant for certain polymer/solvent pairs, and would result in thinner films at higher angular velocities due to the higher shear rate. For $\alpha > -0.5$ the author suggests that the phenomenon is possibly caused by the effect of fluid inertia. For low concentrations (viscosities) and high angular velocities, the lubrication theory described by Lawrence[37] does not give a good prediction, causing the derived exponent to be less negative ($\alpha > -0.5$).

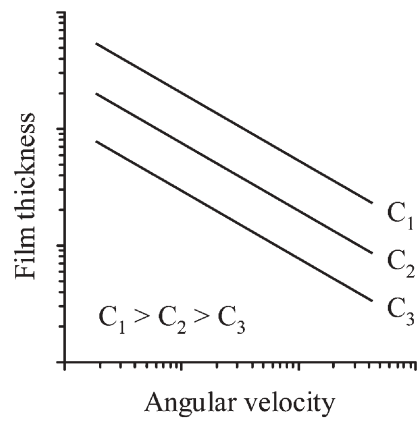

Fig. 2 Schematic of the relation between film thickness, angular velocity and concentration (C_n) in a spin-coating process. The same relation applies for viscosity.

The initial solution viscosity, η_0, is, amongst other parameters, incorporated in the constant k_1 (eqn. (1)). Eqn. (1) can thus be expanded to eqn. (2).[43]

$$h = k_2 \eta_0^{\beta} \omega^{\alpha} \quad (2)$$

The exponent, β, to the initial solution viscosity is typically observed to be in the range 0.29–0.39 for polymer solutions.[27,40,41,43]

Spangler *et al.*[43] used the expression given by eqn. (2) and found the exponents α and β to be fairly independent of the polymer/solvent systems studied. However, the proportionality coefficient, k_2, varied significantly. It was suggested that information about the polymer/solvent interactions is possibly incorporated in k_2 (eqn. (2)).

Solvent evaporation. In early attempts to model the spin-coating process the solvent evaporation was neglected,[25–31] which led to models that were less consistent with experimental observations compared to more recent models that incorporate a wider range of parameters.[32–37] Solvent evaporation changes the physical and thus the rheological properties of the solution during the coating process, especially if the latent heat of evaporation of the solvent is large. This can decrease the temperature (“chilling”) causing the solution properties to change (*e.g.* solvent volatility) and induce non-Newtonian behavior such as elasticity and shear thinning.

Chen[41] has studied the effect of solvent evaporation on spin-coating of polymer solutions. The effect of heat transfer in addition to momentum transfer (fluid flow) and mass transfer (solvent evaporation) was included. The film thickness was quantitatively correlated with the relative rate of solvent evaporation, the solution viscosity, and the angular velocity using solvents with significantly different volatilities. Eqn. (2) was expanded with an additional term related to the physical properties of the solvent, eqn. (3).

$$h = k_3 (E\lambda/C_p)^{\gamma} \eta_0^{\beta} \omega^{\alpha} \quad (3)$$

E is the (average) evaporation rate, λ is the latent heat of evaporation, C_p is the heat capacity of the solvent, and k_3 is a proportional constant. The exponents that correlated best with the experimental results were $\alpha = -0.5$, $\beta = 0.36$ and $\gamma = 0.60$ (poly-(vinyl butyral), PVB, and cellulose dissolved in acetone, butanone and cyclohexanone). The α and β exponents are consistent with literature values.[27,32,36,38–40,41,43] A similar model was derived for aqueous solutions, where the only difference is the $(E\lambda/C_p)$ term that was substituted with (1 – RH), where RH is the relative humidity. The correlation (eqn. (3)) was taken to suggest that, for a given angular velocity, the same film thickness could be obtained by using a low viscosity solution of a highly volatile solvent or a high viscosity solution of a low volatility solvent.

Solute diffusivity. Lawrence[37] challenged the conclusions made by Chen[41] by stating that the model lacks detailed theoretical work provided by his own work. The model by Lawrence[37] (eqn. (4)) is also an expansion of eqn. (2), but the model differs from other theoretical models by also having solute diffusivity incorporated.

$$h = k_4 C_0 (\eta_0 \Delta_0)^{\beta'} \omega^{\alpha} \quad (4)$$

k_4 is a number of order unity (changes slightly with the choice of model for diffusivity and viscosity), C_0 is the initial polymer concentration, and Δ_0 is the solute

diffusivity. The exponent for the angular velocity was found to be $\alpha = -0.5$ while the exponent for the viscosity and diffusivity part was determined as $\beta' = 0.25$. In this model (eqn. (4)) η_0 and Δ_0 increase with C_0 for small concentrations, *i.e.* increasing C_0 should result in a thicker film, and increasing the angular velocity should result in a thinner film. The only problem in considering diffusivity in the model is the lack of diffusivity data for even the most common polymer/solvent pairs.

Bornside *et al.*[36] proposed a model extending the work by Lawrence[37] who assumed the concentration in the bulk to be constant, *i.e.* only varying at a boundary layer adjacent to the free surface. In the model by Bornside *et al.*[36] no assumptions on the vertical (in-depth) variation of solute concentrations are made. Bornside *et al.*[36] predicts the formation of a so-called solid ''skin'' at the free surface (skinning), and that defects in the film could occur if the convective flow is not completed when the skin starts to form. The skinning process can be restricted by partially saturating the space (atmosphere) above the solution coated rotating disc with solvent vapor, or by using a binary-solvent system, *i.e.* containing both a high- and a low-volatility solvent. Finally, Bornside *et al.*[36] found temperature variations during spin-coating to be negligible, which contradicts the result from other work where a significant chilling effect was observed.[38,41] Bornside *et al.*[36] did not correlate the various process parameters with film thickness, as shown in eqns. (1)–(4).

Solvent volatility. Work described in the literature qualitatively relates polymer film thickness with the volatility of the solvent.[41,43] Highly volatile solvents results in thicker films at a given polymer concentration and initial viscosity compared to low volatility solvents.

Morphology of thin-films

The effect of interfacial interactions on film properties. In a polymer film there are two interfaces, the polymer/substrate interface and the polymer/air interface (the free surface). If the polymer and the substrate are compatible the interaction between polymer chain segments and the substrate will be strong causing the mobility of the chain segments in the vicinity of the substrate to be impeded, causing the properties to be affected in that layer (close to the substrate).[44–46] At the free surface it is well-established that the mobility of chain segments is higher compared to the rest of the system due to larger configurational freedom. Dynamic cooperative effects are believed to extend the effect of higher mobility at the surface to a finite distance below the surface, which is proposed to be independent of both film thickness and temperature.[47–49] The liquid film is thus likely to possess local layer properties at the polymer/substrate interface, in the bulk film, and at the free surface, which contributes an inherent asymmetry in the film structure. For small film thicknesses, the interfacial interactions will become more dominant due to the large surface-to-volume ratio and affect the average properties of the entire polymer film accordingly. Recent work exploits designed polymer/substrate interactions to engineer the micromorphology of the resulting polymer film (*vide infra*).

Glass transition temperature. The glass transition temperature (T_g) is the most studied property of thin-films, which is a manifestation of its scientific and technological importance.[44–75] For a decrease in film thickness, T_g has been observed to either decrease or increase depending on the polymer/substrate compatibility.[45–62] The higher chain segment mobility in the surface layers will reduce the T_g in these

layers, and will consequently contribute by lowering the average T_g for the film. If the polymer is compatible with the substrate, that is, interacting with the substrate, the chain segment mobility will be inhibited, and consequently contribute by increasing the average T_g of the film. Forrest *et al.*[60,68] compared supported (asymmetrical film structure) and non-supported (symmetrical film structure) films, and observed that the reduction in T_g for non-supported films were much larger, which supports the fact that polymer/substrate interactions influence the average T_g of the film.

Based on the Michaelis–Menten equation Kim *et al.*[45] proposed a model to estimate T_g in polymer thin-films, eqn. (5).

$$T_g(h) = T_{g,bulk}\frac{h(2k_5 + h)}{(\sigma + h)^2} \quad (5)$$

$T_g(h)$ is the estimated T_g at a film thickness of h, $T_{g,bulk}$ is the T_g for the bulk polymer (*i.e.* at an infinitely large film thickness), σ is the statistical segment length of the polymer, k_5 is a measure of the influence of the polymer/substrate interactions on the average T_g of the film. This may be found by fitting eqn. (5) with experimental T_g *vs.* film thickness data. The model is based on continuous multilayers, *i.e.* many continuous layers with a different T_g associated with each layer. The T_g of the layer facing air is the lowest, T_g's for the underlying layers increase gradually until the layer facing the substrate is reached, which has the largest T_g. Long and Lequeux[46] proposed a different model for systems with strongly interacting substrates where domains of fast and slow dynamics are considered in the glass transition regime (*i.e.* heterogeneous dynamics). Their model considers a critical density separating fast dynamics at high density and slow dynamics at low density. The model describes T_g in terms of the statistical segment length of the polymer, a universal exponent and a parameter which is a measure of the average number of monomers in a domain.

Effect of molecular weight on phase separation of block copolymer films. When the repulsion between incompatible segments of a diblock copolymer (A and B) becomes sufficiently strong phase separation occurs, *i.e.* microdomains rich in one segment type (*e.g.*, A embedded in B) are formed. According to Leibler[76] the state of the phase is only determined by two parameters: (i) The volume fraction of component A (B) and (ii) the product χN, where N is the number of monomers in the copolymer and χ is the Flory parameter[77] (eqn. (6)).

$$\chi = \frac{\varepsilon_{AB} - 0.5(\varepsilon_{AA} + \varepsilon_{BB})}{kT} \quad (6)$$

ε is the interaction energy between two monomers (AA, BB or AB), k is the Boltzmann constant, and T is the temperature. According to de Gennes[48] the critical point of phase separation corresponds to $\chi N = 2$. For a volume fraction between 0.3 and 0.7 the system will phase separate when the product χN is in the range 10–15, and since the Flory parameter[77] is usually $\sim$0.1 for many monomer pairs, phase separation is not expected to occur when $N < \sim 100$, *i.e.* for low molecular weights. Leibler[76] suggested that the inherent minimal size of the microdomains is determined by χN. The kinetics of the ordering of the microdomains limits the maximal size of the microdomains, *i.e.* for higher molecular weights the kinetics slows down. χ is independent of the molecular weight, and since the ability to phase separate increases with χN, it follows that increasing N facilitates phase separation. However, the

subsequent alignment of the microdomains normal to the surface requires coordinated motions of numerous chains, which is a slow process for high N values. Thus, for an increase in molecular weight, the film will approach a non-equilibrium state resulting in a decreased ability to form ordered microdomains. Furthermore, an increase in molecular weight will increase the domain size and the center-to-center distance between microdomains enriched in one type of polymer block.

Controlling aggregate formation in spin-coated polymer films. Shi *et al.*[13] have performed a systematic study of how spin-coating conditions affect the morphology of polymer thin films and how this influences the electronic and photonic properties of the film. The change in properties is believed to be related to formation of aggregates in the polymer solution. Aggregation is caused by short-range interchain attraction forces, which are negligible for diluted solutions, *i.e.* the polymer chains are isolated. For increasing concentration the interchain forces become significant and the polymer coils starts to entangle to form so-called "loose aggregates" that turns into even more entangled so-called "strong aggregates" at higher concentrations. The morphology of the spin-coated thin-film is expected to depend on angular velocity when the centrifugal force is comparable to the cohesive force of the solution, *i.e.* the viscosity of the polymer solution should, to some degree, reflect the intermolecular forces. Shi *et al.*[13] plotted the reduced viscosity of a polymer solution against the concentration. Fig. 3 is a schematic of that plot.

At low concentrations (Fig. 3(a)) the plot is linear, the intermolecular interactions are negligible and the solution has an intrinsic viscosity. For high concentrations (Fig. 3(c)) the plot is linear but with a steeper slope, *i.e.* higher viscosity. The interchain forces are strong in this concentration regime, resulting in strong aggregates. At the intermediate concentration range (Fig. 3(b)) the plot is curved, which corresponds to the concentration regime for loose aggregation of the polymer chains. The actual location of this intermediate regime is dependent on molecular weight and solvent. In this intermediate regime the morphology (aggregation state of the polymer film) is influenced by angular velocity enabling control of the electronic and photonic properties of the polymer film.

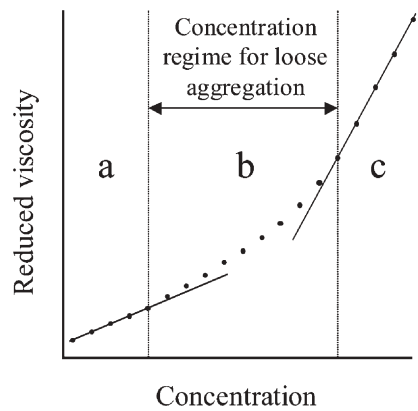

Fig. 3 Schematic of the relation between reduced viscosity and concentration for a polymer solution. (a) Concentration regime for no aggregation. (b) Concentration regime for loose aggregation. (c) Concentration regime for strong aggregation.

Effect of solvent on surface topography

Spangler *et al.*[43] studied the effect of solvent on the surface topography. It was found that both solvent volatility and polymer/solvent interactions affect the surface topography of spin-coated polymer films. Spangler *et al.*[43] classified the compatibility of the polymer/solvent pair as either "good" or "poor", which was suggested to be related to the degree of coiling of the polymer chain in solution. For a good solvent the interactions between polymer and solvent are energetically favorable, *i.e.* the interactions are more favorable than the polymer/polymer and the solvent/solvent interactions, causing the polymer chain to expand. Spangler *et al.*[43] found that for solutions of comparable volatilities only good solvents produce uniform polymer films, and when only good solvents were used, only the solvents with low volatilities produce uniform polymer films. Spangler *et al.*[43] extracted information about the solvent ability by experimentally determining the Mark–Houwink–Sakurada coefficients and exponents, which relates the intrinsic viscosity of a polymer solution to the viscosity average molecular weight (*vide infra*) of the polymer. The exponent is related to the degree of polymer chain expansion in the solvent, and it was empirically determined that the exponent varies from 0.5 (poor solvent) to 0.8 (very good solvent). Graessley[78] has proposed an expression that can approximate the entanglement concentration, eqn. (7).

$$C_e = \rho M_c / M \tag{7}$$

C_e is the entanglement concentration in solution, ρ is the bulk polymer density, M_c is the critical molecular weight at which polymer entanglements in a melt phase become sufficiently strong to contribute significantly to viscosity and M is the molecular weight of the polymer.

Lai[38] also described the effect of solvent on, among other parameters, the surface appearance. The solvent compatibility was alternatively described in terms of solubility parameters, but the conclusions were consistent with the findings of Spangler *et al.*[43]

Effect of molecular weight and dispersity on film thickness

Spangler *et al.*[43] studied the effect of molecular weight and dispersity of the polymer on the film thickness. The dispersity of a polymer is defined as the M_w/M_n ratio, where M_w is the weight average molecular weight and M_n is the number average molecular weight. Based on their experimental results it was concluded that neither M_w nor M_n are the controlling parameters with respect to the film thickness. Instead, the so-called viscosity average molecular weight M_v (eqn. (8)) was proposed to be the controlling molecular weight parameter for the film thickness.

$$M_v = (\sum w_i M_i^{\delta})^{1/\delta} \tag{8}$$

δ is the Mark–Houwink–Sakurada exponent, w_i is the weight fraction of the ith component and M_i is the molecular weight of the ith component. M_v is thus related to the type of solvent (through the parameter δ) and to the molecular weight distribution. Weill and Dechenaux[42] also considered the effect of molecular weight and dispersity on the film thickness, but found M_w to be the controlling factor, which disagrees with the work by Spangler *et al.*[43] These contradicting results have not been resolved.

Shear thinning

Based on the model from Emslie *et al.*,[25] Acrivos *et al.*[26] considered the effect of shear thinning. Acrivos *et al.*[26] analyzed the flow of a power-law fluid and concluded that the rate of thinning is greater near the edge of the disc compared to the center of the disc. This result was not consistent with experimental observations for shear-thinning liquids. Lawrence[37] explains this inconsistency by the erroneous assumption that the viscosity is related to the shear rate by a power-law dependence.

Effect of a transverse magnetic field and non-uniform rotation on surface topography and the rate of film thinning

Dandapat and Layek[79] made a numeric study of the effect of a transverse magnetic field and a non-uniform rotation on spin-coating. By using a finite-difference technique and assuming a planar interface Dandapat and Layek[79] concluded/predicted that an initial impulsive rotation followed by an accelerated angular velocity until the desired film thickness was obtained, will increase the rate of thinning. Furthermore, it was concluded that increasing the angular velocity could decrease the likelihood of hard skinning commonly observed in spin-coating. Finally, Dandapat and Layek[79] suggested that a transverse magnetic field would stabilize the liquid flow in the spin-coating process resulting in suppressed non-uniformities on the film surface.

3 Preparation

Experimental conditions

The preparation of spin-coated polymer films was partly discussed in the previous section. In the following important aspects regarding preparation in order to obtain an optimal polymer film is summarized.

During application of the polymer solution the disc should either be static or rotating at a low angular velocity, followed by rapid acceleration of the angular velocity. Higher polymer concentrations or viscosities result in thicker films, and higher angular velocities results in thinner films. Thus the thickness of the polymer film can be controlled by the concentration or the angular velocity. The size of the rotating substrate is typically up to $\text{Ø} \geqslant 30$ cm, and the thickness of the polymer film is typically in the range from a submonolayer (where degree of surface coverage is a more appropriate term) up to several hundreds of micrometers. The choice of solvent is important. Higher solvent volatilities results in thicker films at a given initial concentration and initial viscosity. The solvent can also be so highly volatile that chilling effects become dominant which results in non-uniformities. Furthermore, greater solvent/polymer compatibility results in more uniform films, *i.e.* less topographical variation in the resulting polymer film surface. The undesirable skinning process, which can cause defects in the film, can be prevented or reduced by partially saturating the atmosphere above the rotating disc by solvent vapor, or by using a multi-component solvent. The outcome of the spin-coating process is not only influenced by the angular velocity and the physical properties of the solution, but can, in addition, be very sensitive to parameters such as temperature, airflow velocity (see Fig. 1), relative humidity and thermal surroundings for the evaporating solvent (heat transfer). Thus in order to perform systematic studies or reproduce polymer films, it is necessary to obtain a fixed set of operational conditions for a given spin-coating apparatus.

Alternative preparation techniques for polymer films

The controllability of the spin-coating process is excellent when it comes to creating a well-defined film with a homogeneous lateral and vertical polymer distribution. However, the spin-coating process is limited to planar substrates, which limits the applicability of the process. Other related techniques are therefore often considered. In the following various alternatives are described and compared to the spin-coating technique.

Dip-coating[80–82]**.** The dip-coating technique is a crude version of the spin-coating technique. In dip-coating the substrate is immersed in a polymer solution and then withdrawn. If the substrate is planar a fairly well-defined polymer film is obtained. The film thickness can be controlled by the withdrawal velocity and by the concentration or viscosity. For non-planar substrates the controllability is lower, *e.g.* the film thickness will not be homogeneous.

Flow-coating[83,84]**.** The flow-coating technique resembles dip-coating, but the polymer solution is poured and guided over the substrate instead of dipping the substrate into the solution. The film thickness can be controlled by the angle of inclination of the substrate and the concentration or viscosity of the polymer solution. The controllability and applicability of flow-coating is similar to that of dip-coating.

Spray-coating[85,86]**.** The spray-coating technique is widely used in industrial applications. A polymer solution is sprayed creating an aerosol of the polymer solution, which is directed towards the substrate where the polymer solution is deposited. The solvent partly evaporates during spraying and the remaining solvent evaporates after deposition. Compared to dip-coating the technique is very fast, but for non-planar substrates (irregularly shaped objects) the controllability of the film thickness is, like dip-coating, low. Controlling the droplet size of the aerosol can to a certain extent control the homogeneity of the polymer film.

Thermal spray-coating[85,87,88]**.** Thermal spray-coating is a solvent-free alternative to spin-coating. Polymer powder is exposed to a heat source (*e.g.* plasma or flame) and the resulting particles are sprayed onto a preheated substrate. The film thickness is controlled by the number of times the substrate is sprayed. The homogeneity is partly controlled by the particle size. The technique can be used on irregularly shaped objects, but the controllability is low compared to spin-coating on planar substrates.

Plasma polymerization[89,90]**.** Plasma polymerization has become a widely developed and applicable technique. A monomer (typically mixed with argon) is introduced into a vacuum chamber. A field is applied between two electrodes crating a plasma of chemically active species (activated molecules, radicals, ions and electrons). The species react with each other and with the substrate of the object placed in the chamber, resulting in the formation of a plasma polymerized thin-film. The plasma polymerization product is covalently bonded to the substrate, and the cross-linking between the chains and between the chains and the substrate prevents mobilization. Controlling the experimental conditions can control the thickness and the homogeneity of the film. Plasma polymerization can be applied to planar surfaces as well as to irregularly shaped objects. However, it has the significant drawback of being a

vacuum technique, which is comparatively slow and complicated for production purposes, and it is only to some extent possible to control the chemistry of the plasma-polymerized film. The inherent crosslinking of the resulting polymer layer may also be incompatible with further chemical patterning processes, *e.g.* photo- or electron-lithography.

Pulsed laser deposition (PLD)[91]. PLD is a solvent-free ultra-high vacuum (UHV) technique. A rotating polymer target situated in a UHV chamber is heated by a laser beam, causing evaporation of polymer particles and further absorption of laser light resulting in plasma formation and expansion. The plasma is then deposited on the substrate situated in the direction of the plasma. The drawbacks are similar to that of plasma polymerization, *i.e.* being a vacuum technique and having a fairly low chemical controllability due to thermal and possibly photochemical degradation products.

Grafting. Polymers possessing reactive functional groups (*e.g.* carboxyl-terminated) can be grafted onto a substrate (*e.g.* a silicon surface), often *via* a spacer (*e.g.* 3-glycidoxypropyltrimethoxysilane) that chemically anchors the polymer to the substrate.[92] It is possible to produce fairly thick polymer films (several hundreds of nanometres), which can be controlled by the molecular weight and the grafting density. For high degree of grafting and/or thick films the film will dominantly possess its intrinsic polymer properties. An advantage of grafting is that the polymer is immobilized on the surface, a useful property in, for example, implant coatings. The fact that the coating is restricted to only a monolayer will be a disadvantage in some applications.

4 Applications

The range of polymers applied by spin-coating in the literature is vast. This review will therefore only consider applications where the spin-coating process and the substrate/solution interactions are deliberately engineered to obtain particular properties of the resulting polymer films. Such properties may be particular micromorphologies, alignment, or ultrastructural characteristics not otherwise accessible through other methods of preparation.

Microelectronics

The use of spin-coating in microelectronics is so widespread and versatile that it would be too overwhelming to attempt to describe all applications published in recent years, so only selected examples with relevance to spin-coating from different fields of microelectronics is described, *e.g.* comparative spin-coating/drop-cast studies or studies involving variation of the spin-coating parameters in order to control polymer thin-film properties. Emphasis is put on spin-coated semiconducting conjugated polymers that are being developed for thin-film transistors, light-emitting diodes and photovoltaic cells.

Organic field-effect transistors (organic FETs). FETs based on organic semiconductors are used in applications such as active matrix displays and logic circuits. Spin-coating is one of the methods used to apply the organic semiconductor layer on the FET device. The morphology of the applied film plays an important role in FET

applications; the molecular ordering influences the field-effect mobility, which is a vital parameter in FETs. Mobilities of $\sim$0.1 $cm^2\ V^{-1}\ s^{-1}$ are considered to be efficient, however, mobilities above 0.1 $cm^2\ V^{-1}\ s^{-1}$ have been observed for polycrystalline or single-crystalline molecular films.[93] Pentacene films have been shown to exhibit the highest mobilities (1–3 $cm^2\ V^{-1}\ s^{-1}$).[10] Much work has been put into optimizing the mobility that is limited by the hopping process, which is affected by the degree of order, *i.e.* charge transport is impeded by amorphous domains. Thus, the upper limit must be the mobility in a perfectly ordered single-crystal. Polymers have excellent film forming and mechanical properties, but it is, compared to molecular films, very difficult to control the molecular ordering of the polymer chains. Certain solution-processed self-organized conjugated polymers form complex microstructures consisting of typically 10-nm microcrystalline domains embedded in an amorphous matrix. It is desirable to gain information about the correlation between polymer microstructure and FET carrier mobility.[1]

Poly(3-hexylthiophene), P3HT, is a well-studied p-type semiconducting polymer that has self-organizing properties to form microcrystalline structures.[1–6,8] A lot of effort has been put into improving the mobility through optimization of device preparation, *e.g.* choice of solvent,[94] dielectric treatments[1] and deposition method.[95] Sirringhaus *et al.*[1–3] investigated the correlation between microstructures and charge carrier mobilities in high-mobility, self-organized FETs of P3HT. The P3HT films were prepared by spin-coating and drop-casting using various molecular weights (M_w = 28 kg mol^{-1}, M_w/M_n = 1.4, M_w = 126 and 175 kg mol^{-1}, M_w/M_n = 2.5–2.7). Substrates made from doped n^+-Si wafers with a 230-nm thick SiO_2 gate insulator layer were made hydrophobic by a hexamethyldisilazane treatment (promotes self-organization) and subsequently spin-coated from 0.8% (w/w) chloroform solutions at 2000 rpm producing film thicknesses of 70–100 nm. Equivalent substrates were drop-cast from a $\sim$0.05% (w/w) chloroform solution producing $\sim$1-μm thick films. The P3HT films prepared by drop-casting exhibited charge carrier mobilities that was a hundred fold larger than the spin-coated P3HT films. From X-ray diffraction measurements it was found that the two preparation methods resulted in two lamella microstructures, *i.e.* two different orientations of ordered P3HT domains relative to the substrate. In the spin-coated films conjugated lamellae and the direction of π–π stacking are oriented normal to the substrate, and in the drop-casted films the orientation is parallel to the substrate. Furthermore, it was found that the FET mobility is critically affected by regioregularity (composition of head-to-head and head-to-tail monomer connections) and molecular weight. In summary, Sirringhaus *et al.*[1–3] demonstrated a clear correlation between the preferential orientation of ordered microcrystalline domains and FET mobility for P3HT.

Krebs *et al.*[6] demonstrated that vacuum ultraviolet (VUV) spectroscopy can be used as an alternative to X-ray diffraction with respect to differentiating between the orientations of ordered P3HT domains relative to the substrate. Highly regioregular P3HT (M_w = 87 kg mol^{-1}) was spin-coated or drop-casted from a 1 mg mL^{-1} chloroform solution onto lithium discs producing film thicknesses of $\sim$180 nm. A large difference in the VUV absorption spectra was observed depending on spin-coating or drop-casting were employed. The spin-coated P3HT film has absorption maxima at 129 and 147 nm that are significantly less intense for the drop-casted film. The two absorption bands at 129 and 147 nm are assigned to the σ–σ* transition from the C–H and C–C bonds in the alkyl chain. Krebs *et al.*[6] concluded that the VUV absorption properties of the σ–σ* transitions are highly anisotropic and very

sensitive to ordered P3HT domains relative to the substrate, and can thus be used to determine the resulting orientation of a given sample preparation if the polymer organization is known from for example X-ray diffraction.

It has been shown that properties such as molecular weight and deposition method are important factors for the microstructure, and thus for obtaining an optimal mobility. The use of spin-coating in general lowers the mobility compared to drop-casting. For spin-coating the solvent evaporation is fast compared to drop-casting, which leaves little time for the polymer chains to align. Chang *et al.*[5] used spin-coating to systematically investigate the effect of solvent properties on the mobility of P3HT transistors. Regioregular (RR) P3HT (M_w = 37 kg mol^{-1}, RR = ~98%) was dissolved in various solvents with different evaporation rates (chloroform, thiophene, xylene, cyclohexylbenzene and 1,2,4-trichlorobenzene) producing solutions of 10 mg mL^{-1}. The substrate consisting of doped n$^+$-Si wafers with a 200-nm thick SiO_2 gate insulator layer were made hydrophobic by a hexamethyldisilazane or perfluorodecyltrichlorosilane treatment, and subsequently spin-coated at 1500 rpm, and annealed at 100 °C for 10 h under vacuum producing P3HT films of 20–60 nm. It was found that the field-effect mobilities vary significantly with the boiling points of the solvent, suggesting that the boiling point is a critical parameter for the polymer crystallization process. The lowest mobilities were observed for chloroform having the lowest boiling point (60.5–61.5 °C), and the highest mobility was observed for 1,2,4-trichlorobenzene having the highest boiling point (218–219 °C). The mobility for 1,2,4-trichlorobenzene was 0.12 cm^2 V^{-1} s^{-1}, which is ten-fold higher than the corresponding value for chloroform. The P3HT films were observed to dry within seconds when chloroform was used, while it took 5–10 min when 1,2,4-trichlorobenzene was used. It was suggested that the polymer molecules can self-organize over a long time to form the thermodynamically favored structure, which corresponds to the microstructure reported for the film prepared by drop-casting. It was concluded that the advantage of using a high-boiling solvent is the combined effect of homogeneity of the spin-coating process and the microstructure of the drop-casting process.

In earlier work Geens *et al.*[7] obtained results that were consistent with the findings of Chang *et al.*[5] Geens *et al.*[7] investigated the effect of spin-coating solvent on the field-effect hole mobility of poly(2-methoxy-5-(3′,7′-dimethyloctyloxy)-1,4-phenylenevinylene) (MDMO-PPV) and found that spin-coating using chlorobenzene as a solvent produced a higher mobility than if toluene was used. The difference is manifested in the different degree of interchain aggregation introduced by a solvent induced modification of the film morphology.

Kline *et al.*[8] studied the effect of molecular weight on field-effect mobility of regioregular P3HT films that were prepared by spin-coating using various molecular weights (M_w = 3.2–36.5 kg mol^{-1}, M_w/M_n = 1.4–1.9). Substrates consistent of doped n$^+$-Si wafers with a 230-nm thick SiO_2 gate insulator layer were made hydrophobic by a hexamethyldisilazane treatment and subsequently spin-coated from 0.5% (w/w) chloroform solutions at 2500 rpm in nitrogen atmosphere producing film thicknesses of 30–60 nm. The mobility was observed to steadily increase with molecular weight from 1.7 × 10^{-6} cm^2 V^{-1} s^{-1} (3.2 kg mol^{-1}) to 9.4 × 10^{-3} cm^2 V^{-1} s^{-1} (36.5 kg mol^{-1}), which was taken to suggest that the molecular weight has a significant effect on the way that the chains pack on each other, *i.e.* there is a better interconnectivity of the polymer network for higher molecular weights. It was concluded that the results did not suggest that disordered films are

intrinsically better than highly crystalline films, but rather demonstrate that factors other than crystallinity can have a significant effect on the mobility. Finally, no mobility saturation or declination was observed, which was taken to suggest that even higher mobilities could be obtained by employing longer polymer chains.

Salleo *et al.*[9] studied the dielectric interface by studying the effect of a self-assembled monolayer of various organic trichlorosilanes between the gate dielectric and the semiconductor in polymeric thin-film transistors, and compared spin-coating with drop-casting. Gate electrodes made of doped n^+-Si wafers with 100 nm of thermally grown SiO_2 were immersed in various organic trichlorosilane solutions (octadecyl-, 7-octenyl-, tridecafluoro-1,1,2,2-tetrahydrooctyl- and benzyltrichlorosilane, 5–10 mM in heptane or hexadecane) in order to form self-assembled monolayers. Poly(9,9-dioctylfluorene-co-bithiophene) (F8T2) films were spin-coated or drop-casted on the derivatized gate electrode surfaces from a $\sim$0.5% (w/w) solution in xylene. By comparing non-derivatized gate electrodes with derivatized gate electrodes it was found that the self-assembled monolayer causes the mobility to increase. The mobilities obtained from the drop-cast samples were observed to be similar to those obtained from spin-coating. This is inconsistent with the findings for P3HT suggesting that other factors are in play for F8T2. The result was taken to indicate that the increase in mobility is not related to macroscopic quantities such as polarity or surface energy, but rather related to certain self-assembled monolayer structures. The most significant effect was observed for octadecyltrichlorosilane that demonstrated a twenty-fold increase in mobility ($1.5 \pm 0.5 \times 10^{-2}$ cm^2 V^{-1} s^{-1}). It was suggested that the presence of long alkane chains (or aromatic rings) enable interactions with similar features in F8T2 *via* induced-dipole dispersion forces. It was concluded that the increase in mobility is caused by another mechanism than the one in the liquid crystalline phase of F8T2.

As is evident from previous discussions much work is focused on optimizing the mobility in organic thin-film transistors by considering different semiconductor materials, the morphology of the semiconductor material and the physical-chemical properties of the gate electrode substrate. Klauk *et al.*[10] demonstrated that using polymeric gate dielectric materials significantly improves the mobility. Gate electrodes made of doped n^+-Si wafers with 100 nm of thermally grown SiO_2 were either not treated, or treated with octadecyltrichlorosilane, or spin-coated with a solution of poly(4-vinylphenol-co-2-hydroxyethylmethacrylate) in *N*-methylpyrrolidinone or spin-coated with a solution of poly(4-vinylphenol) and poly(melamine-co-formaldehyde) in propylene glycol monomethyl ether acetate. After curing the spin-coated films resulted in a gate dielectric layer of a poly(4-vinylphenol-co-2-hydroxyethylmethacrylate) (380 nm) and a layer of cross-linked poly(4-vinylphenol) (260 nm). All gate dielectric substrates were then applied with a layer of semiconducting material consistent of thermally evaporated pentacene. The lowest carrier mobility was observed for the non-treated gate dielectric substrate (0.4 cm^2 V^{-1} s^{-1}). The thin-film transistor with the octadecyltrichlorosilane treated gate dielectric substrate showed an increased mobility (1.0 cm^2 V^{-1} s^{-1}). The co-polymer gate dielectric film caused the mobility to increase to 2.9 cm^2 V^{-1} s^{-1}, and the cross-linked film resulted in a mobility of 3.0 cm^2 V^{-1} s^{-1}, which must be considered as a very high mobility. Klauk *et al.*[10] concluded that the use of spin-coated polymeric gate dielectrics in the fabrication of organic thin-film transistors could lead to simpler processing, lower fabrication costs and improved electrical performance.

Organic light-emitting diodes (OLEDs). Burroughes *et al.*[11] were the first to successfully fabricate a polymer LED using poly(*p*-phenylenevinylene). Since then there has been a widespread research interest in improving the overall performance of LED devices, *i.e.* to optimize the electrical and photonic semiconducting properties. Spin-coating is the most common method to form uniform thin-films of these materials. The spin-coating conditions control the film morphology and the polymer chain aggregation, which are vital parameters that affect the electrical and photonic semiconducting properties.

Corcoran *et al.*[12] demonstrated that it is possible to improve the LED performance by controlling the morphology in conjugated polymer blends. Poly(9,9-dioctyl-fluorene-co-benzothiadiazole) (F8BT) acting as the electron-transporting species and poly(9,9-dioctylfluorene-co-*N*-(4-butylphenyl)diphenylamine) (TFB) acting as the hole-transporting species were dissolved in various solvents (chloroform, xylene and isodurene) to produce 1:1 blend solutions of 15 mg mL^{-1}. Substrates consistent of indium tin oxide (ITO) coated with a 30-nm layer of poly(ethylene dioxythiophene) doped with polystyrene sulfonic acid (PEDOT:PSS) were spin-coated with the polymer blend solutions to produce 100 nm thick polymer films that were subsequently annealed at 200 °C for 12 h. Corcoran *et al.*[12] observed that xylene solution resulted in large-scale lateral phase separation (5–10 μm diameter), and chloroform solution produce fine-scale lateral phase separation in the nanometer range. The isodurene solution cause vertical phase separation with a F8BT-rich top layer. The device made from isodurene solution was observed to be 25% more efficient than the one made from xylene solution and 100% more efficient than the one made from chloroform solution. The difference in efficiencies is attributed to the interfacial areas, *i.e.* the efficiency increases for larger interfacial areas. However, this effect should be balanced against current leakage, which becomes significant if continuous pathways between the electrodes are formed.

Shi *et al.*[13] have performed a systematic study of how spin-coating conditions affect the morphology of polymer thin-film, and how this influences the electronic and photonic properties of a LED device. PEDOT:PSS/ITO was used as an anode and poly(2-methoxy-5-(2′-ethylhexyloxy)-1, 4-phenylene vinylene) (MEH-PPV) was used as the semiconductor material. Solutions of MEH-PPV ($M_w = \sim 1000$ kg mol^{-1}) were spin-coated on the PEDOT:PSS/ITO using various angular velocities, concentrations and solvents. From a UV-VIS absorption study of the polymer thin films it was observed that increasing the angular velocity or decreasing the concentration caused a red-shift at the wavelength for maximal absorption. Furthermore, the angular velocity dependence on the red-shift was found to disappear for concentrations higher than 1% (w/w) or lower than 0.4% (w/w). These results were reproduced with different solvents (cyclohexanone, tetrahydrofuran, chloroform, *p*-xylene, *etc.*). Shi *et al.*[13] suggested that the phenomenon is related to formation of aggregates in the polymer solution (*vide supra*), which explains the correlation between the angular velocity and the red-shift in a specific concentration regime that disappeared at higher concentrations, *i.e.* at higher concentrations the centrifugal forces are insufficient to break the aggregates apart, and the high degree of entanglement will decrease the conjugation of the polymer backbone. For lower concentrations loose aggregates are formed, which are more readily separated by the centrifugal force (and the radial flowing of solvent) resulting in a more extended conformation that will increase the conjugation of the polymer backbone causing a red-shift. The high-end of the concentration regime for loose aggregation is supposed

to result in the best device performance. At very low concentrations the polymer chains are easily stretched to the extended form, and since the polymer chains are isolated the angular velocity does no longer affect the absorption wavelength. Shi *et al.*[13] furthermore performed a study of electroluminescence (EL) and photoluminescence (PL) on the spin-coated films. At high angular velocities the resulting devices had a strong yellow EL emission peak and a weak read shoulder. The yellow EL emission was suggested to originate from a single-chain exciton from the more extended polymer chains. At lower angular velocities the spectrum red-shifts and the red emission peak increases. The yellow emission dominates in the low concentration regime and red emission dominates in the high concentration regime. In the intermediate concentration regime the emission spectra are dependent on the angular velocity. The effect of the angular velocity on the emission spectra were observed when using aromatic solvents (and cyclohexanone). For non-aromatic solvents the dependency is more complicated suggesting that solvation effects play an important role in the morphology of spin-coated polymer films. The solvation effect was found to be more significant at high concentrations. The aromatic polymer backbone is believed to be more readily solvated by aromatic solvents than the alkyl side chains causing the strands of MEH-PPV to aggregate lengthwise in the form of a spiral cylinder with the alkyl side chains pointing radially inwards. In non-aromatic solvents MEH-PPV is suggested to have a twisted conformation. Thus, for aromatic solvents the conformation will be more planar, *i.e.* more conjugated, and for non-aromatic solvents the polymer chains are suggested to be more tightly coiled (less conjugated). Shi *et al.*[13] found the orange–red devices to exhibit higher (30–80%) quantum efficiencies compared to the yellow devices. This result was valid for all studied solvents and was independent of film thickness (50–150 nm). It was then argued that since the red emissive devices have different absorption and emission spectra, different quantum efficiency and different fluorescence decay lifetime relative to that of a single chain exciton, the red emissive species is most likely an interchain excimer species. Finally, it was concluded that in order to improve the quantum efficiency and emission color of a LED device it is necessary to control the polymer aggregation (*via* spin-coating parameters) in such that the rate of formation of the emissive species is maximized and the less emissive species is minimized.

Photovoltaic cells. Some work has been done in recent years on photovoltaic cells with respect to studying the effect of spin-coating parameters, or comparative studies involving alternative film preparation techniques.[14,15]

When polymeric semiconductor materials absorb light, excitons are created. If the exciton dissociation mechanism is sufficiently effective charge separation becomes possible, resulting in free charges in the conjugated polymer, which is a prerequisite for charge transport. Interfaces between certain materials with different electron affinities and ionization potentials are known to facilitate exciton dissociation. Controlling the nanoscale phase-separation of blends of polymers exhibiting these properties will thus affect the charge transport properties, which enables optimization of the photovoltaic device.[14,15] Varying the spin-coating parameters can control the nanoscale phase-separation mechanisms. The efficiency of a photovoltaic device is measured by the external quantum efficiency (EQE), which is defined as electrons collected per incident photon.

In a series of articles Arias *et al.*[14,15] investigated aspects of morphology, controlled by spin-coating conditions, on the performance of photovoltaic devices.

One article explored vertically segregated polymer-blend photovoltaic thin-film structures through surface-mediated solution processing. The compositional structure normal to the plane of the film is important for optimizing the charge transport in the device. The polymer-blend consisted of equal amounts of the hole acceptor poly(9,9′-dioctylfluorene-co-bis-*N*,*N*′-(4-butylphenyl)-bis-*N*,*N*′-phenyl-1,4-phenylenediamine) (PFB) and the electron acceptor F8BT, which were dissolved in isodurene and xylene at a concentration of 14 mg L^{-1}. The solutions were spin-coated on an ITO/PEDOT:PSS substrate for only 2 s in order to suppress instabilities, lateral phase separation and increase the transformation rate, which produced 90-nm thick films. In both cases the higher phase was found to be F8BT. The less volatile and more viscous isodurene solution produced a much more continuous F8BT layer. To further improve the stability of the layered structure, the PEDOT surface was modified with self assembled monolayers of 7-octenyltrichlorosilane before spin-coating, which was performed under different solvent evaporation conditions: (i) xylene, (ii) xylene with a xylene-rich atmosphere and (iii) isodurene. The xylene solution caused lateral phase separation of the same order as on the unmodified PEDOT and produced the lowest EQE. For the xylene solution in a xylene-rich atmosphere the lateral phase separation is less pronounced, *i.e.* more continuous, causing an increase in EQE. The isodurene solution produced a smooth continuous surface suggesting a layered structure. The device prepared with isodurene showed an efficiency that was 14 times better than the device prepared from xylene.

In earlier work Arias *et al.*[15] studied the same semiconducting materials systematically by another approach. Varying the composition of PFB and F8BT revealed that a 1:1 composition produces the highest EQE. Furthermore, both the blends and the homopolymers were examined in xylene or chloroform. The photovoltaic response was systematically investigated by varying the experimental conditions for preparation of the polymer films. Three procedures were utilized: (i) spin-coating at room temperature, (ii) drop-casting under a controlled atmosphere and (iii) spin-coating on a heated substrate. The homopolymers were dissolved in xylene or chloroform to a concentration of 14 mg mL^{-1} and used as is or to produce 1:1 mixtures. The polymer solutions were applied directly on an ITO substrate where after an aluminium electrode was deposited. The blend solutions resulted in higher efficiencies than the homopolymers, as expected. The chloroform solutions demonstrated higher EQEs compared to the more slowly evaporating xylene solution. This was taken to suggest that the rapid evaporation impede the rearrangement of the polymer chains and quenches the phase-separation on a scale similar to the exciton diffusion length (tens of nanometers). When employing drop-casting the transformation is observed to be much slower, resulting in phase-separation on a much larger scale, *i.e.* low EQEs compared to spin-coating. Heating the substrate (40 °C) causes the evaporation rate to increase, resulting in significantly increased EQEs. Arias *et al.*[15] concluded that by controlling the experimental conditions for preparation of the polymer films, it was possible to control the phase-separation length scales from tens of nanometers to tens of microns resulting in photovoltaic efficiencies from 0.5 to 4%.

Sensors

Spin-coating is widely applied in the field of sensor technology. There is a significant amount of interest in developing optical sensors for the detection of oxygen. In

optics-based oxygen sensors the optical response from a film (*e.g.* changes in luminescence or absorbance) is correlated with the oxygen concentration. Eaton[16] constructed a colorimetric oxygen sensor based on dye redox chemistry (2,6-dichloroindophenol) in the presence of fructose and base in a thin polymer film (ethyl cellulose). The polymer film acts an encapsulation agent. Polymer solutions of ethyl cellulose were prepared containing the necessary components and spin-coated for 3 s at 3690 rpm onto glass slides producing homogeneous films of $\sim$15 μm thickness (after solvent evaporation). In absence of oxygen the sensor film is colorless but turns blue when exposed to oxygen. The response time when changing the oxygen concentration was found to be fast ($\sim$20 s), but increased upon prolonged cycling.

The oxygen sensor agent can be based on principles other than redox chemistry. Oxygen sensors based on oxygen binders are well known; they are either biological or synthetic. Douglas and Eaton[17] developed an oxygen sensor based on complexation with platinum and palladium octaethylporphyrins encapsulated in various polymers. The oxygen sensors were prepared by spin-coating a mixture of lumophore solution and polymer solution. It was found that the sensitivity of the sensor not only depends on whether platinum or palladium is used, but also depends on the choice of polymer. This was explained by the difference in oxygen permeability of the polymers used.

Mirkhalaf and Schiffrin[18] studied metal-ion sensing by encapsulating dithiazone and its dicarboxylic derivative in hydrophilic and hydrophobic polymers. The metal-ion specific ligands were dissolved in agarose or polystyrene (PS) solution containing an agent to improve conductivity and porosity of the sensing film. The polymers were then spin-coated as gels on electrode surfaces to produce a membrane film with metal-ion sensing capabilities. During the metal-ion complexation the optical properties change, which is monitored by surface plasmon resonance analysis.

The field of relative humidity sensing has many practical applications in the fields of medicine, meteorology, agriculture and process control. Penza and Anisimkin[19] fabricated a humidity sensor based on surface acoustic waves (SAW). A 42 MHz SAW delay line was spin-coated for 30 s at 6000–7000 rpm with a drop of polyvinyl alcohol (M_w = 10–100 kg mol^{-1}) solution producing a $\sim$1 μm thick film that was subsequently cured at 50 °C in air for 30 min. The film thickness was found to vary with $\pm$10%, which was proposed to be due to the electrostatic charges on the dielectric SAW substrate. When water is interacting with the poly(vinyl alcohol) film there will be a response in the acoustic parameters (phase, frequency, attenuation) that combined with a calibration will provide the relative humidity. The relative humidity range from 10 to 90% was examined and it was found that the sensitivity decreases with the sensing temperature below the glass transition temperature of the poly(vinyl alcohol) film (T_g = $\sim$70 °C).

Protective coatings

Protective coatings are used widely for various industrial applications, such as protection against UV light, corrosion, humidity and scratching. The largest (in number of items produced) industrial application for protective coatings is data storage, both magnetic storage in hard disc drives and optical storage in compact discs (CDs), digital versatile discs (DVDs), and next-generation high density DVDs (HD-DVDs). The development of ever-higher capacities is manifested in the use of

ever-smaller dimensions in parameters such as wavelength, substrate thickness, surface spot diameter and free working distance. The small dimensions makes the readout of the recording layer more susceptible to errors due to dust and scratches on the surface. The layer that covers the metal layer is usually polycarbonate or UV-curable resin, which have a low surface hardness and hence are more susceptible to scratches. There is thus an ever-increasing demand for scratch protection as the development in optical recording accelerates. Among the possible methods to coat CDs and DVDs spin-coating has proven to be the most advantageous, having good adhesive strength, low processing cost and small residual focusing error. The traditional protective coating consists of a UV-curable resin of photosensitive monomers, oligomers, photo-initiator and various additives.

Chang *et al.*[20] investigated a possible coating for the next-generation HD-DVDs. One of the goals was to obtain a protective coating with improved protective properties, *e.g.* towards scratching and static electricity. Chang *et al.*[20] composed the UV-curable resin from a trifunctional aliphatic urethane acrylate that functions as the oligomer. A polyether–siloxane copolymer and a non-ionic fluorine-containing surfactant were used to improve the slip properties, which additionally will improve the scratch resistance. Conductive ITO particles of 3–50 nm were added as an antistatic agent. All the components including solvent were mixed together in a one-step process and subsequently spin-coated on a polycarbonate substrate. There is great demand for precision in film thickness and homogeneity, which was achieved by controlling the spin-coating parameters. Chang *et al.*[20] managed to produce a total film thickness (cover layer and protective coating) of 100 ± 2 μm, which satisfies the requirement of still being able to focus the light on the surface. Chang *et al.*[20] observed that when the proportion of electro-conductive ITO particles increases the surface resistivity decreases. Less antistatic effect was observed below 5% of ITO, and above 8% the homogeneity and transparency begins to be affected. The loss in transmittance (at 405 nm) due to the protective layer is only $\sim$2%, which is within the acceptable range. Chang *et al.*[20] demonstrated that it is possible to design improved protective coatings for next-generation HD-DVDs without significantly degrading the optical properties.

Optical coatings

Spin-coating is an obvious technique for applications in the field of optical coatings, *e.g.* optical sensors, emissive displays, light-emitting diodes, integrated optical circuits among many others. For anti-reflection applications low-refractive indices are essential to improve the light transmission for various applications. The research in antireflection coatings is, however, somewhat inhibited due to lack of materials with sufficiently low refractive indices. Walheim *et al.*[22] overcame this by demonstrating an antireflection coating that produces surfaces with high optical transmission that was based on a nanoporous polymer film. The immiscible polymers PS and poly(methyl methacrylate) (PMMA) were dissolved in tetrahydrofuran and spin-coated onto a glass substrate where phase separation takes place resulting in the formation of domains of each of the polymers. The glass slide was then washed with cyclohexane that selectively dissolves the PS producing a nanoporous film. Maximizing the volume ratio of the pores will minimize the refractive index, which is desirable for broadband antireflection coatings. The pore parameters are controlled by the preparation parameters, *e.g.* polymer composition in the solution and spin-coating parameters.

Membranes

The development of porous polymer membranes has expanded strongly during the last decade and includes a whole range of preparation techniques. A special, more sophisticated, class of porous polymer membranes includes cylindrical pores of uniform size, which are typically produced by imprint lithography or from block copolymers. Block copolymers can phase separate into ordered, periodic arrays of spheres, cylinders or lamellae. When the desired domain structure (film morphology) is obtained the minor component can be removed producing an ordered array of micro/nano-pores. Control of the pore size, pore size distribution and pore density partially controls the membrane properties. Thus, to control the membrane properties it is advantageous to control the alignment and ordering of the microdomains into arrays oriented normal to the surface of the film. For ultra-thin films the interfacial interactions are controllable and affect the alignment of the cylindrical domains aligned normal to the film surface.

Xu *et al.*[24] studied the influence of molecular weight on nanoporous polymer films. Diblock copolymers of PS and PMMA with a constant volume fraction (of PMMA) of 0.3, but with varying molecular weights (M_w = 42–295 kg mol^{-1}) were used to produce membranes with different pore characteristics. The PS-PMMA block copolymers were dissolved in toluene and spin-coated on two surfaces (balanced with respect to their interfacial interactions): (i) a ~6 nm layer of a random PS/PMMA copolymer brush and on (ii) a hydrogen passivated silicon substrate. The result was ~30 nm thin films that was then heated to 170 °C for 48 h in order to orient the cylindrical domains. Additionally, thick films were produced by spin-coating 10% (w/v) solutions of the block copolymers onto a silicon substrate. A layer of poly(dimethylsiloxane), PDMS, was spin-coated on top of the block copolymer film, which acted as a buffer layer between the block copolymer and an upper electrode. An electric field was applied during annealing to facilitate the alignment of the cylindrical domains. After cooling, the electrode was removed and the PDMS was removed by dissolution in hexane, leaving a smooth film of the block copolymer. The minor component (PMMA) was then removed from the thin and thick films by irradiation with 25 J cm^{-2} deep ultraviolet light that causes the PS to cross-link and the PMMA to degrade. Finally, the degradation products are removed with acetic acid and water. It was found that the size of the microdomains could, within some limitations, be controlled by the molecular weight of the diblock copolymers. For all methods of preparation an increase in molecular weight was observed to increase the domain size and the center-to-center distance between the cylindrical microdomains. Xu *et al.*[24] obtained arrays of hexagonally packed, cylindrical microdomains with resulting pore diameters in the range between 14 and 50 nm with the lattice period varying from 24 to 89 nm.

Yan *et al.*[23] used the concept of replica molding against a template to produce monodisperse cylindrical pores in polymer membranes. PS (bimodal distribution, M_w = 200 and 4 kg mol^{-1}) was dissolved in toluene to produce a 12.5% (w/w) solution that was then spin-coated on silicon wafers and subsequently baked at 90 °C for 60 s to remove residual solvent. A glass plate coated with chromium was placed ~5 μm above the PS film (*via* spacers). By applying a voltage of 200 V across the gap for several minutes while heating at 120 °C, an ensemble of pillars is formed. The structure is then fixated/frozen by lowering the temperature. The electrodes are then separated with most of the PS pillars adhering to the chromium substrate that function as the mold. Nylon 6/6 dissolved in formic acid was then put on the mold

and the solvent was evaporated for 1 h. The nylon 6/6 end-caps of the PS pillars were removed by fast solvent dissolution and evaporation. The PS pillars were then removed by dissolution in tetrahydrofuran for ~5 h, producing a nylon 6/6 film with a pore diameter size of 5.0 ± 1.4 μm. The pore size can be controlled by adjusting the pillar formation conditions, *e.g.* PS film thickness and electric field, or by decreasing the pore diameter by plating the walls with metal. Membranes based on the concept of replica molding against a template are associated with high liquid permeabilities and high size selectivities.

Morphology

A tremendous amount of work related to morphology of spin-coated polymer films is described in the literature, so in order to limit the description of this area, only very recent work is described.

It has been very popular to study morphology of spin-coated immiscible polymer blends (PMMA and PS in particular). The effect of molecular weight on the film morphology and thermal stability of spin-coated PMMA and PS blends were studied by Li *et al.*[96] by the use of atomic force microscopy (AFM) and X-ray photoelectron spectroscopy (XPS). Li *et al.*[96] dissolved a mixture (1:1 w/w) of PMMA and PS in toluene using various molecular weights of PS, which were spin-coated (2000 rpm at room temperature for an unknown amount of time) and finally dried in vacuum at 50 °C for 10 h, resulting in a film thickness range between 70 and 90 nm. Three types of morphology were observed when the molecular weight of PS was varied from 2.9 to 129 kg mol^{-1}: (i) a nanophase separated morphology, (ii) a PMMA cellular or network-like morphology where the meshes are filled with PS, and (iii) a morphology that is described as a "sea-island like" morphology. This result was taken to suggest that the film morphology can be controlled by varying the molecular weight. When the aforementioned samples were annealed two morphology changes was observed: (i) for molecular weights of PS less than 4 kg mol^{-1} a top layer rich in PS was formed on top of a PMMA layer that was in contact with the substrate, and (ii) for molecular weights higher than 4 kg mol^{-1} the PS forms domains on top of the PMMA layer.

Pham and Green[44] studied the morphology of spin-coated miscible polymer blends, in particular, the effect of film thickness and composition on the effective T_g. Solutions with varying compositions of tetramethyl bisphenol-A polycarbonate, TMPC, (M_w = 37.9 kg mol^{-1}, M_w/M_n = 2.75) and PS (M_w = 49 kg mol^{-1}, M_w/M_n = 1.06) were prepared using toluene. The solutions were spin-coated onto silicon with varying solution concentrations and angular velocities resulting in film thicknesses in the range between ~20 and ~200 nm, which were then annealed at 200 °C for a few hours in vacuum to relax the film and to remove residual solvent. The thickness was then measured by ellipsometry while simultaneously heating the sample. The resulting temperature *vs.* film thickness plots all consisted of two intersecting straight lines, *i.e.* a glassy and a rubbery region where the intersect corresponds to the effective T_g (residing between that of each of the polymers). The effective T_g was obtained from a variety of film thicknesses that enabled the effective T_g to be plotted against film thickness. In addition, the same procedure was performed with pure TMPC films. For the TMPC film, T_g was observed to increase for a decreasing film thickness, an observation that was explained by the strong interaction of TMPC with the substrate *via* hydrogen bonding. The mobility in the vicinity of the substrate thus becomes impeded and the local T_g will be higher than

the bulk T_g. For thinner films the contribution of this elevated T_g becomes more significant, *i.e.* increases the average T_g in the film. By contrast, the effective T_g for the polymer blends was observed to decrease with decreasing film thickness. This was explained from the fact that the more polar TMPC interacts more strongly with the polar substrate, but the bulk and the surface is enriched with PS that have a lower T_g, and since the PS mobility at the free surface is intrinsically higher than the TMPC chains interacting with the substrate, the T_g contribution from the surface is expected to dominate, *i.e.* decreasing the average T_g of the film. In addition, Pham and Green[44] found that the effective T_g for the polymer blends become independent of film thickness for thicker films (the interfaces do not contribute significantly), and also found that while the T_g of the bulk blends exhibited large negative deviations from additivity with composition, this was (practically) not the case for thin film blends.

When polymers are grafted *via* a spacer onto a substrate with only one end, and if the distance between the grafted chains is smaller than the average end-to-end distance of the polymer chain, then the coating/film is in the regime of a so-called polymer brush. Minko *et al.*[92] produced adaptive (binary) polymer brushes. The first step was to chemisorb a spacer onto a silicon surface, which was done by 3-glycidoxypropyl trimethoxysilane dissolved in toluene that was left for 16 h at room temperature. The next step consisted of spin-coating carboxyl-terminated PS (various molecular weights and dispersities) dissolved in toluene on top of the spacer resulting in a 50 $\pm$ 5 nm film. Then the system was heated at 150 °C in vacuum for different amounts of time, after which the polymer is expected to have reacted with the spacer. The next step was to spin-coat carboxyl-terminated poly(2-vinylpyridine) on top of the aforementioned sample with subsequent equivalent heating. The result is a binary adaptive polymer brush that have interesting properties. Due to the different properties of the two polymers (*e.g.* hydrophobic and hydrophilic) the morphology can be affected by external stimuli (*e.g.* solvent and temperature). Minko *et al.*[92] found that the morphology changes can be monitored by AFM, X-ray reflectivity and contact angle measurements. The binary brush was shown to switch from hydrophilic to hydrophobic (and *vice versa*) when exposed to an appropriate solvent. This was suggested to be useful in a variety of technical and biomaterial applications.

The majority of work in the field of morphology of spin-coated polymer films has focused on immiscible polymer blends, whereas the morphology of sub-monolayers of homopolymers has received little attention. Norrman *et al.*[97] studied the morphology and quantitative aspects of spin-coated poly(vinyl chloride), PVC, (M_w = 80 kg mol^{-1}, M_w/M_n = 1.7) and PMMA (M_w = 70 kg mol^{-1}, M_w/M_n = 2.09) solutions on silicon substrates. A broad concentration range (1–10^4 μg mL^{-1}) was used that enabled formation of submonolayers as well as fully covering films. In Fig. 4 selected AFM images show the lateral distribution of PVC at various spin-coating concentrations.

When correlating AFM, XPS and time-of-flight secondary ion mass spectrometry (TOF-SIMS) data with spin-coating concentration, interesting plots were revealed that all had a distinct break in them (Fig. 5). This phenomenon was explained from morphology changes.

At low concentrations, the deposited polymer material is heterogeneously distributed in the plane of the film as well as vertically to the substrate, resulting in relatively high hillocks (with very gentle sidewall slopes) distributed over a limited

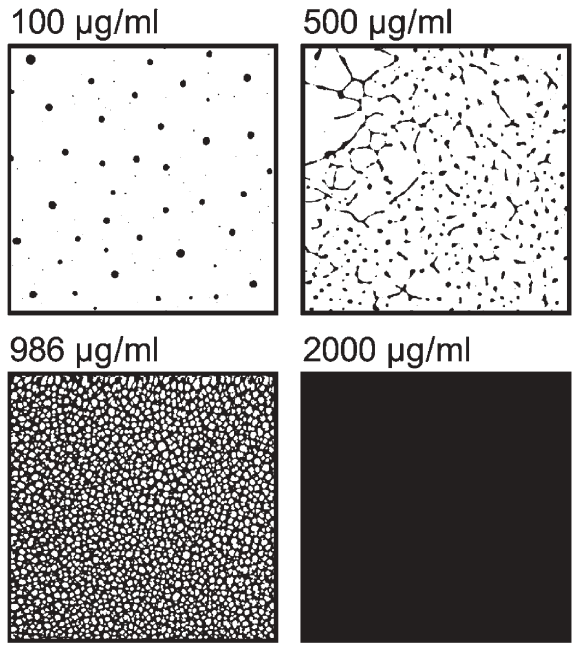

Fig. 4 AFM images of spin-coated PVC on silicon using various spin-coating concentrations. Each area corresponds to 50 × 50 μm^2. The images have been processed by a threshold function to show PVC in black and the substrate in white. The PVC (M_w = 80 kg mol^{-1}, M_w/M_n = 1.7) was dissolved in a mixture of cyclohexanone and tetrahydrofuran (3:2 v/v) and spin-coated at 4000 rpm for 60 s.

surface area. At higher concentrations, when the network starts to form, it is more favorable to distribute the polymer in the lateral plane rather than normal to the surface plane, resulting in a relatively thin network with a large degree of surface coverage. This explains the breaks in the plots shown in Fig. 5 (the corresponding AFM measured degree of surface coverage plots are qualitatively equivalent). The break corresponds to incipient network formation. When integrating the deposited volume the expected power-law dependence is observed between the amount of polymer deposited and the concentration in the spin-coating solution. Neither polymer shows an increase in the amount deposited on the surface at the concentration that corresponds to incipient network formation, consistent with the suggested morphology changes.

Petri[74] studied the competitive interactions between polymer, solvent and substrate and the effect on the morphology of spin-coated polymer films. PS (M_w = ~200 kg mol^{-1}), PVC (M_w = ~80 kg mol^{-1}) and PVB (M_w = ~40 kg mol^{-1}) were dissolved in all possible combinations with toluene and tetrahydrofuran producing 10 mg mL^{-1} solutions. The solutions were spin-coated at 3000 rpm for 30 s at room temperature onto silicon and subsequently dried with nitrogen. For PS dissolved in toluene the film thickness was measured to be 50 ± 2 nm, while the PVB dissolved in tetrahydrofuran resulted in a film thickness of 99 ± 5 nm (other combinations produced films of a quality/morphology that prevents thickness measurement). Petri[74] concluded that when the interaction energy between the solvent and the substrate is dominating over the interaction between the polymer and the substrate,

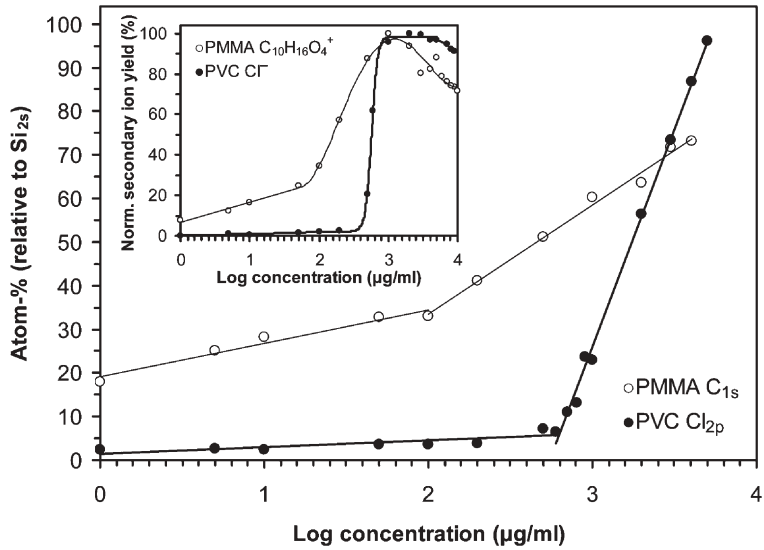

Fig. 5 C/(C + Si) and Cl/(Cl + Si) compositions determined by XPS *vs.* spin-coating concentration. The inset is the normalized TOF-SIMS secondary ion yield versus concentration. The dimer signal was used as a marker for PMMA.

the result is segregation and consequently a rough film is formed. By contrast, if the interaction between the polymer and the substrate is energetically favored, homogeneous films are formed.

Annealing effects on film thickness, thermal expansivity and glass transition temperature was investigated by Kanaya *et al.*[75] by the use of neutron reflectrometry. Deuterated PS (M_w = 300 kg mol^{-1}, M_w/M_n = 1.06, T_g = 103 °C) was dissolved in toluene at various concentrations and spin-coated (2000 rpm for an unknown amount of time) on Si(111) producing film thicknesses of 9, 18 and 40 nm. The samples were then either ''weakly'' annealed (80 °C for 12 h) or ''strongly'' annealed (135 °C for 12 h). One of the purposes of the study was to determine if unrelaxed structure caused by either lack of or insufficient annealing could possibly explain the negative expansivity reported elsewhere for very thin films. Kanaya *et al.*[75] found that weakly annealed films exhibit negative expansivity in the glassy state, which disappears if strongly annealed with thickness above 9 nm. This was taken to indicate that the negative expansivity is caused by an unrelaxed structure. Based on non-equivalent thickness versus temperature curves for the cooling and heating process it was suggested that an additional (slower) relaxation process is in play. This additional slower relaxation process was observed to reduce the film thickness but to have no affect on expansivity in the glassy state.

5 Outlook

Spin-coating as a technique for preparing well-defined polymer thin films has been around for almost a century without much change in the tools employed. Still, a whole range of highly interesting and novel applications in both basic research and industrial development has appeared in the last decade. This can largely be ascribed to the accessibility of novel advanced analysis tools with molecular scale resolution

that can reveal both the surface and internal ultrastructure of the polymer thin films that had hitherto been inaccessible. In basic research, this has, for example, led to new insight into the phenomena governing microphase separation in block copolymer systems as their confinement in one dimension approaches molecular dimensions.

The steeply rising focus on nanotechnology as the next industrial global technology also supports the continued and extended use of a well-proven technology capable of producing nanometer scale objects in one dimension over large areas through a simple process. Nanotechnology can be seen as a shift in focus from bulk properties to interface interactions. This is again reflected in the novel uses of spin-coating during the last decade where engineered interface interactions are exploited to direct internal molecular organization of polymer thin films, resulting in highly anisotropic materials properties. This trend will no doubt be strengthened in the years to come as a response to the academic and industrial demand for ever-higher built-in functionality of "smart materials".

References

1 H. Sirringhaus, N. Tessler and R. H. Friend, *Science*, 1998, **280**, 1741.
2 H. Sirringhaus, P. J. Brown, R. H. Friend, M. M. Nielsen, K. Bechgaard, B. M. W. Langeveld-Voss, A. J. H. Spiering, R. A. J. Janssen, E. W. Meijer, P. Herwig and D. M. de Leeuw, *Nature (London)*, 1999, **401**, 685.
3 H. Sirringhaus, P. J. Brown, R. H. Friend, M. M. Nielsen, K. Bechgaard, B. M. W. Langeveld-Voss, A. J. H. Spiering, R. A. J. Janssen and E. W. Meijer, *Synth. Met.*, 2000, **111–112**, 129.
4 J. J. Apperloo, R. A. J. Janssen, M. M. Nielsen and K. Bechgaard, *Adv. Mater.*, 2000, **12**, 1594.
5 J-F Chang, B. Sun, D. W. Breiby, M. M. Nielsen, T. I. Sølling, M. Giles, I. McCulloch and H. Sirringhaus, *Chem. Mater.*, 2004, **16**, 4772.
6 F. C. Krebs, S. V. Hoffmann and M. Jørgensen, *Synth. Met.*, 2003, **138**, 471.
7 W. Geens, S. E. Shaheen, B. Wessling, C. J. Brabec, J. Poortmans and N. S. Sariciftci, *Org. Electron.*, 2002, **3**, 105.
8 R. J. Kline, M. D. McGehee, E. N. Kadnikova, J. Liu and J. M. J. Fréchet, *Adv. Mater.*, 2003, **15**, 1519.
9 A. Salleo, M. L. Chabinyc, M. S. Yang and R. A. Street, *Appl. Phys. Lett.*, 2002, **81**, 4383.
10 H. Klauk, M. Halic, U. Zschieschang, G. Schmid and W. Radlik, *J. Appl. Phys.*, 2002, **92**, 5259.
11 J. H. Burroughes, D. D. C. Bradley, A. R. Brown, R. N. Marks, K. Mackay, R. H. Friend, P. L. Burns and A. B. Holmes, *Nature (London)*, 1990, **347**, 539.
12 M. Corcoran, A. C. Arias, J. S. Kim, J. D. MacKenzie and R. H. Friend, *Appl. Phys. Lett.*, 2003, **82**, 299.
13 Y. Shi, J. Liu and Y. Yang, *J. Appl. Phys.*, 2000, **87**, 4254.
14 A. C. Arias, M. Corcoran, M. Banach, R. H. Friend and J. D. MacKenzie, *Appl. Phys. Lett.*, 2002, **80**, 1695.
15 A. C. Arias, J. D. MacKenzie, R. Stevenson, J. J. M. Halls, M. Inbasekaran, E. P. Woo, D. Richards and R. H. Friend, *Macromolecules*, 2001, **34**, 6005.
16 K. Eaton, *Sens. Actuators B*, 2002, **85**, 42.
17 P. Douglas and K. Eaton, *Sens. Actuators B*, 2002, **82**, 200.
18 F. Mirkhalaf and D. J. Schiffrin, *J. Electroanal. Chem.*, 2000, **484**, 182.
19 M. Penza and V. I. Anisimkin, *Sens. Actuators*, 1999, **76**, 162.
20 D. Chang, D. Yoon, M. Ro, I. Hwang, I. Park and D. Shin, *Jpn. J. Appl. Phys.*, 2003, **42**, 754.
21 P. H. Walker and J. G. Thompson, *Proc. Am. Soc. Test. Mater. (Part 2)*, 1922, **22**, 464.
22 S. Walheim, E. Schäffer, J. Mlynek and U. Steiner, *Science*, 1999, **283**, 520.
23 X. Yan, G. Liu, M. Dickey and C. G. Willson, *Polymer*, 2004, **45**, 8469.
24 T. Xu, H.-C. Kim, J. DeRouchey, C. Seney, C. Levesque, P. Martin, C. M. Stafford and T. P. Russel, *Polymer*, 2001, **42**, 9091.
25 A. G. Emslie, F. T. Bonner and L. G. Peck, *J. Appl. Phys.*, 1958, **29**, 858.
26 A. Acrivos, M. J. Shah and E. E. Peterson, *J. Appl. Phys.*, 1960, **31**, 963.

27 B. D. Washo, *IBM J. Res.*, 1977, **21**, 190.
28 S. A. Jenekhe, *Polym. Eng. Sci.*, 1983, **23**, 830.
29 S. A. Jenekhe and S. B. Schuldt, *Ind. Eng. Chem. Fundam.*, 1984, **23**, 432.
30 S. A. Jenekhe and S. B. Schuldt, *Chem. Eng. Commun.*, 1985, **33**, 135.
31 B. G. Higgins, *Phys. Fluids*, 1986, **29**, 3522.
32 D. Meyerhofer, *J. Appl. Phys.*, 1978, **49**, 3993.
33 S. A. Jenekhe, *Ind. Eng. Chem. Fundam.*, 1984, **23**, 425.
34 W. W. Flack, D. S. Soong, A. T. Bell and D. W. Hess, *J. Appl. Phys.*, 1984, **56**, 1199.
35 P. C. Sukanek, *J. Imag. Technol.*, 1985, **11**, 184.
36 D. E. Bornside, C. W. Macosko and L. E. Scriven, *J. Imag. Technol.*, 1987, **13**, 122.
37 C. J. Lawrence, *Phys. Fluids*, 1988, **31**, 2786.
38 J. H. Lai, *Polym. Eng. Sci.*, 1979, **19**, 1117.
39 F. L. Givens and W. J. Daughton, *J. Electrochem. Soc.*, 1979, **126**, 269.
40 W. J. Daughton and F. L. Givens, *J. Electrochem. Soc.*, 1982, **129**, 173.
41 B. T. Chen, *Polym. Eng. Sci.*, 1983, **23**, 399.
42 A. Weill and E. Dechenaux, *Polym. Eng. Sci.*, 1988, **28**, 945.
43 L. L. Spangler, J. M. Torkelson and J. S. Royal, *Polym. Eng. Sci.*, 1990, **30**, 644.
44 J. Q. Pham and P. F. Green, *J. Chem. Phys.*, 2002, **116**, 5801.
45 J. H. Kim, J. Jang and W.-C. Zin, *Langmuir*, 2001, **17**, 2703.
46 D. Long and F. Lequeux, *Eur. Phys. J. E*, 2001, **4**, 371.
47 W. E. Wallace, D. A. Fischer, K. Efimenko, W.-L. Wu and J. Genzer, *Macromolecules*, 2001, **34**, 5081.
48 P. G. de Gennes, *Eur. Phys. J. E*, 2000, **2**, 201.
49 L. Xie, G. B. DeMaggio, W. E. Frieze, J. DeVries, D. W. Gidley, H. A. Hristov and A. F. Yee, *Phys. Rev. Lett.*, 1995, **74**, 4947.
50 E. K. Lin, W. Wu and S. Satija, *Macromolecules*, 1997, **30**, 7224.
51 E. K. Lin, R. Kolb, S. Satija and W. Wu, *Macromolecules*, 1999, **32**, 3753.
52 K. F. Mansfield and D. N. Theodorou, *Macromolecules*, 1991, **24**, 6283.
53 J. Baschnagel and K. Binder, *Macromolecules*, 1995, **28**, 6808.
54 G. Reiter, *Macromolecules*, 1994, **27**, 3046.
55 J. L. Keddie, R. A. L. Jones and R. A. Cory, *Europhys. Lett.*, 1994, **27**, 59.
56 J. L. Keddie, R. A. L. Jones and R. A. Cory, *Faraday Discuss.*, 1994, **98**, 219.
57 W. E. Wallace, J. H. van Zanten and W. Wu, *Phys. Rev. E: Stat. Phys., Plasmas, Fluids, Relat. Interdiscip.*, 1995, **52**, R3329.
58 J. H. Zanten, W. E. Wallace and W. Wu, *Phys. Rev. E: Stat. Phys., Plasmas, Fluids, Relat. Interdiscip.*, 1996, **53**, R2053.
59 J. A. Forrest, K. Dalnoki-Veress, J. R. Stevens and J. R. Dutcher, *Phys. Rev. Lett.*, 1996, **77**, 4108.
60 J. A. Forrest, K. Dalnoki-Veress and J. R. Dutcher, *Phys. Rev. E: Stat. Phys., Plasmas, Fluids, Relat. Interdiscip.*, 1997, **56**, 5705.
61 Y. Grohens, M. Brogly, C. Labbe, M.-O. David and J. Schultz, *Langmuir*, 1998, **14**, 2929.
62 W. E. Wallace, N. C. Beck Tan, W.-L. Wu and S. Satija, *Chem. Phys.*, 1998, **108**, 3798.
63 G. Beaucage, R. Composto and R. S. Stein, *J. Polym. Sci. Phys. Ed.*, 1993, **31**, 319.
64 W. J. Orts, J. H. van Zanten, W. Wu and S. K. Satija, *Phys. Rev. Lett.*, 1993, **71**, 867.
65 G. Reiter, *Europhys. Lett.*, 1993, **23**, 579.
66 J. L. Keddie and R. A. L. Jones, *Isr. J. Chem.*, 1995, **35**, 21.
67 W. Wu, J. H. van Zanten and W. J. Orts, *Macromolecules*, 1995, **28**, 771.
68 J. A. Forrest, K. Dalnoki-Veress, J. R. Stevens and J. R. Dutcher, *Phys. Rev. Lett.*, 1996, **77**, 2002.
69 C. W. Frank, V. Rao, M. M. Despotopoulou, R. F. W. Pease, W. D. Hinsberg, R. D. Miller and J. F. Rabolt, *Science*, 1996, **273**, 912.
70 G. B. DeMaggio, W. E. Frieze, D. W. Gidley, M. Zhu, H. A. Hristov and A. F. Yee, *Phys. Rev. Lett.*, 1997, **78**, 1524.
71 G. Kleideiter, O. Prucker, H. Bock, C. W. Frank, M. D. Lechner and W. Knoll, *Macromol. Symp.*, 1999, **145**, 95.
72 J. A. Forrest and J. Mattsson, *Phys. Rev. E: Stat. Phys., Plasmas, Fluids, Relat. Interdiscip.*, 2000, **61**, R53.
73 G. Reiter and P. G. de Gennes, *Eur. Phys. J. E*, 2001, **6**, 25.
74 D. F. S. Petri, *J. Braz. Chem. Soc.*, 2002, **13**, 695.
75 T. Kanaya, T. Miyazaki, H. Watanable, K. Nishida, H. Yamano, S. Tasaki and D. B. Bucknall, *Polymer*, 2003, **44**, 3769.
76 L. Leibler, *Macromolecules*, 1980, **13**, 1602.

77 P. J. Flory, *Principles of Polymer Chemistry*, Cornell University Press, Ithaca, New York, 1953.
78 W. W. Graessley, *Polymer*, 1980, **21**, 258.
79 B. S. Dandapat and G. C. Layek, *J. Phys. D: Appl. Phys.*, 1999, **32**, 2483.
80 R. R. Willey, *Practical Design and Production of Optical Thin Films*, Marcel Dekker Inc., New York, 2nd edn., 2002.
81 A. R. M. Oliveira and A. J. G. Zarbin, *Quim. Nova*, 2005, **28**, 141.
82 M. Callewaert, J. F. Gohy, C. C. Dupont-Gillain, L. Boulange-Petermann and P. G. Rouxhet, *Surf. Sci.*, 2005, **575**, 125.
83 K. L. Beers, J. F. Douglas, E. J. Amis and A. Karim, *Langmuir*, 2003, **19**, 3935.
84 P. Belleville, C. Bonnin and J. J. Priotton, *J. Sol–Gel Sci. Technol.*, 2000, **19**, 223.
85 D. Y. Ju, V. Ji and H. Gassot, *J. Phys. IV (Proc.)*, 2004, **120**, 381.
86 M. Ichiki, L. Zhang, Z. Yang, T. Ikehara and R. Maeda, *Microsyst. Technol. Micro. Nanosyst. Inf. Storage Processing Syst.*, 2004, **10**, 360.
87 J. Mostaghimi, S. Chandra, R. Ghafouri-Azar and A. Dolatabadi, *Surf. Coat. Technol.*, 2003, **163**, 1.
88 R. Tucker and C. Tucker, *Int. J. Powder Metall.*, 2002, **38**, 45.
89 R. d'Agostino, D. Flamm and O. Auciello, *Plasma Deposition, Treatment and Etching of Polymers*, Academic Press, New York, 1990.
90 H. Yasuda, *Plasma Polymerization*, Academic Press, New York, 1985.
91 R. K. Singh and J. Narayan, *Phys. Rev. B: Condens. Matter*, 1990, **41**, 8843.
92 S. Minko, S. Patil, V. Datsyuk, F. Simon, K.-J. Eichhorn, M. Motornov, D. Usov, I. Tokarev and M. Stamm, *Langmuir*, 2002, **18**, 289.
93 J. G. Laquindanum, H. E. Katz and A. J. Lovinger, *J. Am. Chem. Soc.*, 1998, **120**, 664.
94 Z. Bao, A. Dodabalapur and A. J. Lovinger, *Appl. Phys. Lett.*, 1996, **69**, 4108.
95 G. Wang, J. Swensen, D. Moses and A. J. Heeger, *J. Appl. Phys.*, 2003, **93**, 6137.
96 X. Li, Y. Han and L. An, *Polymer*, 2003, **44**, 8155.
97 K. Norrman, K. B. Haugshøj and N. B. Larsen, *J. Phys. Chem. B*, 2002, **106**, 13114.